2D Image Analysis by Generalized Hilbert Transforms in Conformal Space⋆

Lennart Wietzke, Oliver Fleischmann and Gerald Sommer
`lw@ks.informatik.uni-kiel.de`

Kiel University, Department of Computer Science
Christian-Albrechts-Platz 4, 24118 Kiel, Germany

Abstract. This work presents a novel rotational invariant quadrature filter approach - called *the conformal monogenic signal* - for analyzing i(ntrinsic)1D and i2D local features of any curved 2D signal such as lines, edges, corners and junctions without the use of steering. The *conformal monogenic signal* contains the *monogenic signal* as a special case for i1D signals and combines monogenic scale space, phase, direction/orientation, energy and curvature in one unified algebraic framework. The *conformal monogenic signal* will be theoretically illustrated and motivated in detail by the relation of the 3D Radon transform and the generalized Hilbert transform on the sphere. The main idea is to lift up 2D signals to the higher dimensional conformal space where the signal features can be analyzed with more degrees of freedom. Results of this work are the low computational time complexity, the easy implementation into existing Computer Vision applications and the numerical robustness of determining curvature without the need of any derivatives.

1 Introduction

Low level 2D image analysis is often the first step of many Computer Vision tasks. Therefore *local* signal features such as color information, gradient, curvature, orientation and phase determine the quality of subsequent higher level processing steps. It is important not to lose or to merge any of the original information within the local neighborhood, i.e. to span a orthogonal feature space. In this paper 2D images $f \in L_2(\Omega; \mathbb{R})$ with $\Omega \subset \mathbb{R}^2$ will be locally analyzed on a low level. 2D signals are classified into local regions $N \subseteq \Omega$ of different intrinsic dimension (see figure 1)

$$\text{i0D} := \{ f \in L_2(\Omega; \mathbb{R}) : f(\mathbf{x}_i) = f(\mathbf{x}_j) \ \forall \mathbf{x}_i, \mathbf{x}_j \in N \}$$
$$\text{i1D} := \{ f \in L_2(\Omega; \mathbb{R}) : f(x, y) = g(x \cos \theta + y \sin \theta) \ \forall (x, y) \in N \} - \text{i0D}$$
$$\text{i2D} := L_2(\Omega; \mathbb{R}) - (\text{i0D} \cup \text{i1D}) \ .$$

The assumed local signal model which will be analyzed in this work is defined as a curve which can be locally approximated by a circle with arbitrary orientation

and curvature

$$f(x,y) := a \, \cos\left(\left\|\begin{bmatrix} x \\ y \end{bmatrix} - \frac{1}{\kappa}\begin{bmatrix} \cos\theta \\ \sin\theta \end{bmatrix}\right\| + \phi\right) \in \text{i1D} \cup \text{i2D} \qquad (1)$$

with $a \in \mathbb{R}$ as the local amplitude, $\phi \in [0, 2\pi)$ as the local phase, $\kappa \in \mathbb{R}$ as the local curvature and $\theta \in [0, 2\pi)$ as the local direction/orientation of the signal for $\kappa \neq 0$. For the special case of $\kappa = 0$ the curved 2D signal degrades to an i1D function. Therefore the task is to solve an *inverse problem*, i.e. to determine local features such as amplitude a, phase ϕ, orientation θ and curvature κ of any curved signal such as lines, edges, corners and junctions. One important local structural feature is the phase ϕ which can be calculated by means of the Hilbert transform [1]. Furthermore all signals will be analyzed in *monogenic scale space* [2] since the Hilbert transform can only be interpreted for narrow banded signals consisting of only one frequency $f(x, y; s_s) := \mathcal{P}(x, y; s_s) * f(x, y)$ with $*$ as the convolution operator and s_s as the scale space parameter. The Poisson kernel of the applied low pass filter reads

$$\mathcal{P}(\mathbf{x}) := \mathcal{P}(\mathbf{x}; s_s) := \frac{s_s}{2\pi \left(s_s^2 + \|\mathbf{x}\|^2\right)^{\frac{n+1}{2}}} \quad n \in \mathbb{N}, \, \mathbf{x} \in \mathbb{R}^n \, . \qquad (2)$$
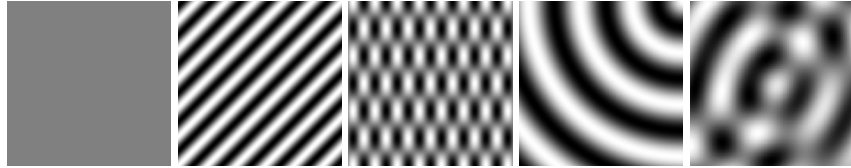

Fig. 1. From left to right: a constant signal (i0D), an arbitrary rotated 1D signal (i1D) and an i2D checkerboard signal consisting of two simple superimposed i1D signals. A curved i2D signal and two superimposed curved i2D signals. Note that all signals displayed here preserve their intrinsic dimension globally.

1.1   Related Work

Phase and energy of 1D signals can be analyzed by the *analytic signal* [1]. The generalization of the analytic signal to multidimensional signal domains has been done by the *monogenic signal* [3]. In case of 2D signals the *monogenic signal* delivers local phase, orientation and energy information restricted to the set of i1D signals. This work presents the generalization of the *monogenic signal* for 2D signals to analyze both i1D and i2D signals in one unified framework. The *conformal monogenic signal* delivers local phase, orientation, energy and curvature for i1D and i2D signals with the *monogenic signal* as a special case.

The *monogenic signal* replaces the classical 1D Hilbert transform of the analytic signal by the generalized Hilbert transform [4]

$$R\{f\}(\mathbf{x}) := (\mathcal{Q} * f)(\mathbf{x}) := (h_n * \mathcal{P} * f)(\mathbf{x}) \quad \mathbf{x} \in \mathbb{R}^n, \; n \in \mathbb{N} - \{1\} \qquad (3)$$

with $\mathcal{Q}$ as the conjugated Poisson kernel and h_n as the generalized Hilbert transform kernel

$$h_n(\mathbf{x}) := \frac{2}{A_{n+1}} \frac{\mathbf{x}}{\|\mathbf{x}\|^{n+1}} \quad \mathbf{x} \in \mathbb{R}^n, \; n \in \mathbb{N} - \{1\} \qquad (4)$$

with A_{n+1} as the surface area of the unit sphere $\mathbb{S}^n$ in Euclidian space $\mathbb{R}^{n+1}$. To enable interpretation of the generalized Hilbert transform, its relation to the Radon transform is the key [5]. The generalized Hilbert transform can be expressed by a concatenation of the Radon transform, the inverse Radon transform and the well known classical 1D Hilbert transform. Note that the relation to the Radon transform is required solely for interpretation and theoretical results. Neither the Radon transform nor its inverse are ever applied to the signal in practice. Instead the generalized Hilbert transformed signal will be determined by convolution in spatial domain and the signal features can be extracted in a rotational invariant way.

2 Generalized Hilbert Transforms in Conformal Space

The feature space of the 2D *monogenic signal* is spanned by phase, orientation and energy information. This restriction correlates to the dimension of the associated 2D Radon space [5]. Therefore, the idea of this work is that the feature space of the 2D signal can only be extended by lifting up the original signal to higher dimensions. This is one of the main ideas of the *conformal monogenic signal*. In the following the 2D monogenic signal will be generalized to analyze also i2D signals by embedding the 2D signal into the 3D conformal space [6]. The 2D generalized Hilbert transform can be expressed by the 2D Radon transform which integrates all function values on lines [7]. This restriction to lines is one of the reasons why the 2D monogenic signal is limited to i1D signals (such as lines and edges) and can not be applied to corners and general curves. To analyze also i2D signals and to measure curvature $\kappa = \frac{1}{\rho}$, a 2D Radon transform which integrates on curved lines (i.e. local circles with radius ρ) is preferable. In 3D domain the Radon transform integrates on planes, although at first sight 3D planes are not related to 2D signals. But the idea is that circles form the intersection of a sphere (with center at $\left[0, 0, \frac{1}{2}\right]$ and radius $\rho = \frac{1}{2}$) and planes passing through the origin $(0, 0, 0)$ of 3D space. Since the generalized Hilbert transform can be extended to any dimension [8] and the 3D generalized Hilbert transform can be expressed by the 3D Radon transform, the 2D signal coordinates must be mapped appropriately to the sphere. This mapping must be conformal (i.e. angle preserving), so that angular feature interpretation of the 3D generalized Hilbert transform in conformal space is still reasonable. Analogous to the line parametrization by $(t, \theta) \in \mathbb{R} \times [0, \pi)$ of the 2D Radon transform

[5], the planes of the 3D Radon transform are uniquely defined by the parameters $(t, \theta, \varphi) \in \mathbb{R} \times [0, 2\pi) \times [0, \pi)$. This new parametrization truly extends the interpretation space of the monogenic signal by one dimension. In contrast to the well known Monge patch embedding known from differential geometry [9], the original 2D signal will now be embedded into the conformal space.
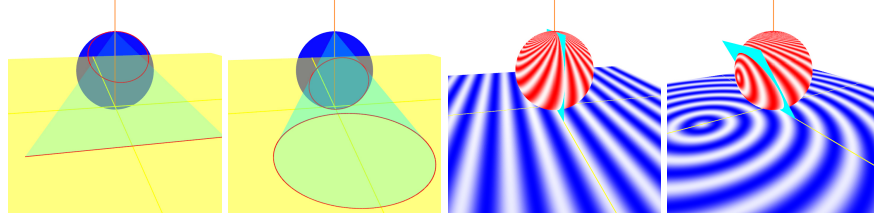

Fig. 2. Lines and circles of the 2D image domain are both mapped to circles on the sphere. Each circle on the sphere is uniquely defined by its parameterized intersection plane in conformal space. The third figure illustrates the monogenic signal as a special case.

2.1   The Conformal Space

The main idea is that the concept of lines in 2D Radon space becomes the concept of planes in 3D Radon space and the more abstract concept of hyperplanes in multidimensional space. These planes determine circles on the sphere in conformal space. Since lines and circles of the 2D signal domain are mapped to circles [6] on the sphere (see figure 2), the integration on these circles determines points in the 3D Radon space. The projection $\mathcal{C}$ known from complex analysis [6] maps the original 2D signal domain to the sphere and can be inverted by $\mathcal{C}^{-1}$

$$\mathcal{C}(x, y) := \frac{1}{x^2 + y^2 + 1} \begin{bmatrix} x \\ y \\ x^2 + y^2 \end{bmatrix}, \quad \mathcal{C}^{-1}(x, y, z) := \frac{1}{1 - z} \begin{bmatrix} x \\ y \end{bmatrix}. \qquad (5)$$

This mapping has the property that the 2D origin $(0, 0)$ of a local coordinate system will be mapped to the south pole $(0, 0, 0)$ of the sphere in conformal space and both $-\infty, +\infty$ will be mapped to the north pole $(0, 0, 1)$ of the sphere. Lines and circles of the 2D signal domain will be mapped to circles on the sphere and can be determined uniquely by planes in 3D conformal space. The integration on these planes corresponds to points (t, θ, φ) in the 3D Radon space.

2.2   3D Radon Transform in Conformal Space

To interpret the *conformal monogenic signal*, the relation to the 3D Radon transform in conformal space must be taken into account. The 3D Radon transform
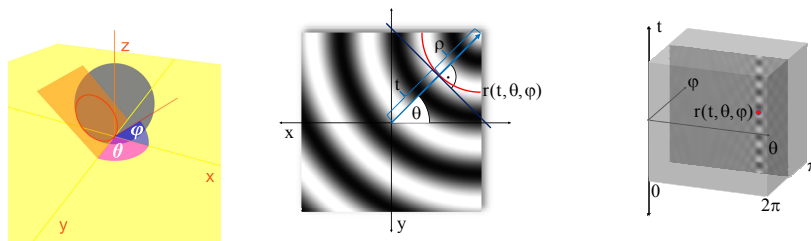
Fig. 3. Left figure: Each $(t = 0, \theta, \varphi)$ parameterized plane can be determined exactly by the generalized Hilbert transforms on the sphere. The interpretation of this parameter set delivers the features such as direction, phase and curvature of the original signal without any steering. Middle figure: Curved i2D signal with orientation θ and curvature $\kappa = \frac{1}{\rho}$. Right figure: Corresponding 3D Radon space representation of the i2D signal spanned by the parameters t, θ and φ. Since the Radon transform on circles directly on the plane of the original 2D signal is not possible, the Radon transform has to be done in higher dimensional 3D conformal space where circles correspond to planes.

is defined as the integral of all function values on the plane (see figure 2) defined by

$$\mathcal{R}\{c\}(t, \theta, \varphi) = \int\limits_{\mathbf{x} \in \mathbb{R}^3} c(\mathbf{x}) \delta_0 (\mathbf{x} \begin{bmatrix} \sin\varphi\cos\theta \\ \sin\varphi\sin\theta \\ \cos\varphi \end{bmatrix} - t) d\mathbf{x} \ . \tag{6}$$

Since the signal is mapped on the sphere and all other points of the conformal space are set to zero, the 3D Radon transform actually sums up all points lying on the intersection of the plane and the sphere. For all planes this intersection can either be empty or a circle. The concept of circles in the conformal 3D Radon transform can be compared with the concept of lines known from the 2D Radon transform. Since lines in the 2D signal domain are also mapped to circles, the *conformal monogenic signal* can analyze i1D as well as curved i2D signals in one single framework. Recall the very important fact that every corner or curve can be locally approximated by a circle. The inverse 3D Radon transform exists and differs from the 2D case such that it is a *local* transformation [10].

$$\mathcal{R}^{-1}\{r\}(0, 0, 0) = -\frac{1}{8\pi^2} \int\limits_{\theta=0}^{2\pi} \int\limits_{\varphi=0}^{\pi} \frac{\partial^2}{\partial t^2} \ r(t, \theta, \varphi)|_{t=0} \ d\varphi \ d\theta \ . \tag{7}$$

That means the generalized Hilbert transform at $(0, 0, 0)$ is completely determined by all planes passing the origin (i.e. $t = 0$). In contrast, the 2D monogenic signal requires all integrals on all lines (t, θ) to reconstruct the original signal at a certain point and is therefore called a *global* transform. This interesting fact turns out from the definition of the inverse 3D Radon transform $\mathcal{R}^{-1}\{\cdot\}$. Therefore, the local features of i1D and i2D signals can be determined by the *conformal monogenic signal* at each test point of the original 2D signal without knowledge of the whole 3D Radon space.

2.3   The Conformal Monogenic Signal

To give the generalized Hilbert transform more degrees of freedom for signal analysis, the original 2D signal will be embedded in a applicable subspace of the 3D conformal space by the mapping

$$c(x, y, z) := \begin{cases} f(\mathcal{C}^{-1}(x, y, z)^T; s_s) & , x^2 + y^2 + \left(z - \frac{1}{2}\right)^2 = \frac{1}{4} \\ 0 & , \text{else} \end{cases} . \tag{8}$$

Thus, the 3D generalized Hilbert transform can be applied to all points on the sphere. The center of convolution in spatial domain is the south pole $(0, 0, 0)$ where the test point of the 2D signal domain meets the sphere. At this point the 3D generalized Hilbert transform will be performed at the origin $(\mathbf{0})$ of the applied local coordinate system for each test point separately. The *conformal monogenic signal* [11] is defined as

$$f_{\text{CMS}}(\mathbf{0}) := [c(\mathbf{0}), R_x\{c\}(\mathbf{0}), R_y\{c\}(\mathbf{0}), R_z\{c\}(\mathbf{0})]^T \tag{9}$$

and can be expressed by the classical 1D Hilbert transform kernel $h_1(\tau) := -\frac{1}{\pi\tau}$ [1], the 3D Radon transform and its inverse analogous to the monogenic signal in 2D [5]

$$\begin{bmatrix} R_x\{c\}(\mathbf{0}) \\ R_y\{c\}(\mathbf{0}) \\ R_z\{c\}(\mathbf{0}) \end{bmatrix} = \begin{bmatrix} \mathcal{R}^{-1} \left\{ \begin{bmatrix} \sin\varphi\cos\theta \\ \sin\varphi\sin\theta \\ \cos\varphi \end{bmatrix} h_1(t) * \mathcal{R}\{c\}(t, \theta, \varphi) \right\} (0, 0, 0) \end{bmatrix} \tag{10}$$

with $*$ as the 1D convolution operator. Compared to the 2D monogenic signal the *conformal monogenic signal* performs a 3D generalized Hilbert transformation in conformal space.
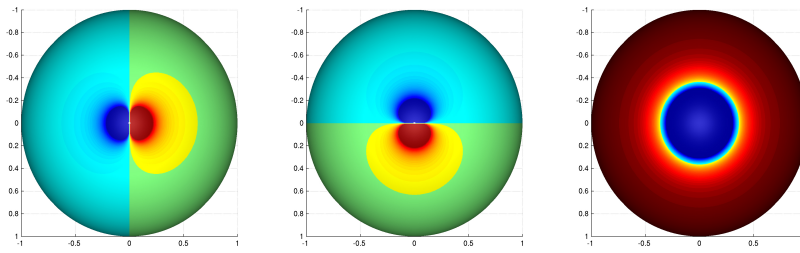

Fig. 4. From left to right: 2D convolution kernels in spatial domain of the *conformal monogenic signal* in x, y and z direction.

3   Interpretation

Analogous to the interpretation of the *monogenic signal* in [5], the parameters of the plane within the 3D Radon space determine the local features of the

curved i2D signal (see figure 2). The *conformal monogenic signal* can be called the generalized monogenic signal for i1D and i2D signals, because the special case of lines and edges can be considered as circles with zero curvature. These lines are mapped to circles passing through the north pole in conformal space. The parameter θ will be interpreted as the orientation in i1D case and naturally
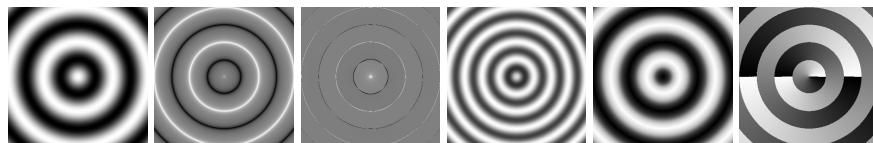

Fig. 5. From left to right: Original synthetic i2D signal $f(x, y) = a \cos(\sqrt{x^2 + y^2} + \phi)$, *conformal monogenic signal* curvature and classical isophote curvature [12], *conformal monogenic signal* energy, phase and direction. Convolution mask size: 11×11 pixels. Rotational invariance and isotropic properties can be clearly seen.

deploys to direction $\theta \in [0, 2\pi)$ for the i2D case

$$\theta = \operatorname{atan2}\left(R_y \{c\} (\mathbf{0}), R_x \{c\} (\mathbf{0})\right) . \tag{11}$$

The energy of the signal is defined by

$$E = a^2 = c^2(\mathbf{0}) + R_x^2 \{c\} (\mathbf{0}) + R_y^2 \{c\} (\mathbf{0}) + R_z^2 \{c\} (\mathbf{0}) . \tag{12}$$

The i1D and i2D curvature phase is defined by

$$\phi = \operatorname{atan2}\left(\sqrt{R_x^2 \{c\} (\mathbf{0}) + R_y^2 \{c\} (\mathbf{0}) + R_z^2 \{c\} (\mathbf{0})}, c(\mathbf{0})\right) . \tag{13}$$

Note that all proofs are analogous to those for the 2D monogenic signal shown in [5].

3.1   Local Isophote Curvature

The parameter φ of the 3D Radon space corresponds to the isophote curvature κ [12] known from differential geometry

$$\varphi = \arctan \frac{\sqrt{R_x^2 \{c\} (\mathbf{0}) + R_y^2 \{c\} (\mathbf{0})}}{R_z \{c\} (\mathbf{0})}, \ \kappa = \frac{-f_{xx} f_y^2 + 2 f_x f_y f_{xy} - f_{yy} f_x^2}{\left(f_x^2 + f_y^2\right)^{\frac{3}{2}}} \tag{14}$$

Proof:
Let be $\gamma(t) := [\rho(\cos\theta + \cos t), \rho(\sin\theta + \sin t)]^T$ with $t \in [0, 2\pi)$ a parametrization of a circle in the 2D plane touching the origin $(0, 0)$ with radius ρ and tangential orientation θ. This circle will be the model for the osculating circle touching
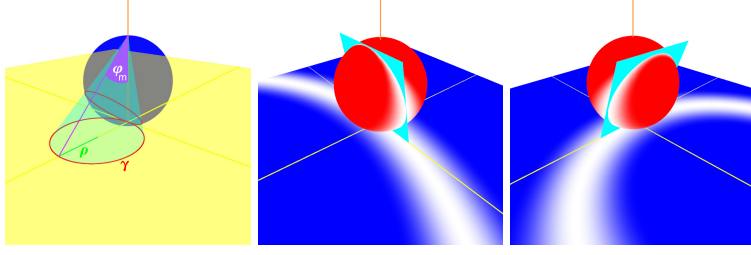
Fig. 6. Left figure: Visualization of the circle described by γ projected to $\mathbb{S}^2(m_S, \rho_S)$. This figure illustrates that $\frac{1}{\kappa} = \rho = \tan \varphi_m$.

the isophote curve of the 2D signal f at the origin $(0,0)$ of the local coordinate system for each test point. Therefore, $f(\gamma(t_1)) = f(\gamma(t_2)) \; \forall t_1, t_2 \in [0, 2\pi)$. Define $\gamma_S(t) := \mathcal{C}(\gamma(t))$ as the projection of γ to the sphere $\mathbb{S}^2(m_S, \rho_S) := \left\{ v \in \mathbb{R}^3 : \|v - m_S\| = \rho_S \right\}$ with the center $m_S = \left[0, 0, \frac{1}{2} \right]^T$ and the radius $\rho_S = \frac{1}{2}$. Furthermore define $f_S(\gamma_S(t)) := f(\mathcal{C}^{-1}(\gamma_S(t)))$. The conjugate Poisson kernel in $\mathbb{R}_+^{n+1}$ reads $\mathcal{Q}(x) := [\mathcal{Q}_x(x), \mathcal{Q}_y(x), \mathcal{Q}_z(x)]^T = (h_3 * \mathcal{P})(x)$ with $R\{f_S\}(\mathbf{x}) = (\mathcal{Q} * f_S)(\mathbf{x})$. The radius ρ of the osculating circle described by the parameterized curve γ reads

$$\rho = \frac{2R_z\{f_S\}(\mathbf{0})}{\sqrt{R_x^2\{f_S\}(\mathbf{0}) + R_y^2\{f_S\}(\mathbf{0})}} \; . \tag{15}$$

Since the values of $f_S(x)$ will only be nonzero for $x \in \mathbb{S}^2(m_S, \rho_S)$, the integration can be restricted to the ball $\mathbb{B}^2(m_S, \rho_S) := \left\{ v \in \mathbb{R}^3 : \|v - m_S\| \leqslant \rho_S \right\}$. Furthermore $f_S(x)$ is only nonzero for the circle projected on the sphere $M := \{\gamma_S(t) : t \in [0, 2\pi)\}$. Now let $\mathbb{S}^2(m, \rho)$ be the sphere whose intersection with $\mathbb{S}^2(m_S, \rho_S)$ results in M. Then the set M is a circle on the surface of $\mathbb{S}^2(m_S, \rho_S)$ and $\mathbb{S}^2(m, \rho)$. The integration over the volumes of $\mathbb{B}^2(m, \rho)$ and $\mathbb{B}^2(m_S, \rho_S)$ will be the same.

$$\int_{x \in \mathbb{R}_+^3} \mathcal{Q}(x) f_S(x) \, dx = \int_{x \in \mathbb{B}^2(m_S, \rho_S)} \mathcal{Q}(x) f_S(x) \, dx = \int_{x \in \mathbb{B}^2(m, \rho)} \mathcal{Q}(x) f_S(x) \, dx$$

According to the results from harmonic analysis [13] the convolution of a function in $\mathbb{R}^n$ with the Poisson kernel $\mathcal{P}$ in upper the half space $\mathbb{R}_+^{n+1}$ results in a harmonic function in $\mathbb{R}_+^{n+1}$. Therefore, $\mathcal{Q}$ is harmonic in $\mathbb{R}_+^{3+1}$. Using the *mean value theorem* for harmonic functions it follows that

$$\int_{x \in \mathbb{B}^2(m, \rho)} \mathcal{Q}(x) \, dx = k \, \mathcal{Q}(m) \tag{16}$$

with the components of $\mathcal{Q}$ written in spherical coordinates

$$\mathcal{Q}(m) = \begin{bmatrix} \mathcal{Q}_x(m) \\ \mathcal{Q}_y(m) \\ \mathcal{Q}_z(m) \end{bmatrix} = \frac{1}{[\|m\|^2 + s_s^2]^2} \begin{bmatrix} \sin \varphi_m \cos \theta_m \\ \sin \varphi_m \sin \theta_m \\ \cos \varphi_m \end{bmatrix} \tag{17}$$

with s_s as the scale space parameter. Since f_S is the signal model for the isophote curve of a signal in the plane, it is a curve consisting of constant values. Therefore, $f_S(x)$ will be constant for all $x \in M$ which results in

$$\int_{x \in \mathbb{B}^2(m,\rho)} \mathcal{Q}(x) f_S(x) \, dx = f_c \int_{x \in \mathbb{B}^2(m,\rho)} \mathcal{Q}(x) \, dx = f_c \, k \, \mathcal{Q}(m) . \qquad (18)$$

With equation (15) it is now possible to determine $\frac{\sin \varphi_m}{\cos \varphi_m}$. Figure 6 illustrates that this is exactly $\frac{\rho}{2 \, \rho_S}$. Since $\rho_S = \frac{1}{2}$ it follows that the radius of the local curvature can be determined by $\rho = \frac{\sin \varphi_m}{2 \cos \varphi_m} = \frac{\sqrt{\mathcal{Q}_x^2(m) + \mathcal{Q}_y^2(m)}}{2 \mathcal{Q}_z(m)}$.

4   Implementation

Although in theory the *conformal monogenic signal* performs a 3D generalized Hilbert transform in conformal space this can be accelerated by simplifying to a faster 2D convolution directly on the sphere. Therefore the following implementation can be done in $O(n^2)$ with n as the convolution mask size in one dimension. Any 2D image can now be analyzed locally at every test point by the following algorithm

```
//Input:  double Image(double x,double y)
//Input:  double x,y (Local pixel test point for analysis)
//Input:  double Coarse > Fine > 0 (Bandpass filter parameters)
//Input:  double Size > 0 (Convolution mask size)
//Output: Direction, Phase, Curvature, Energy
double Coarse=0.2,Fine=0.1,Size=5;//e.g.
double rp=0,rx=0,ry=0,rz=0;
for(double cx = -Size;cx <= Size;cx++)
for(double cy = -Size;cy <= Size;cy++) {
    //Map points (cx,cy) to conformal space (u,v,w)
    double d = pow(cx,2) + pow(cy,2) + 1;
    double u = cx / d, v = cy / d, w = (d - 1) / d;
    //Generalized Hilbert transform in conformal space
    double uvw = pow(u,2) + pow(v,2) + pow(w,2);
    double pf  = pow(pow(Fine  ,2) + uvw,-2);
    double pc  = pow(pow(Coarse,2) + uvw,-2);
    double f   = Image(x + cx,y + cy);
    double c   = f * (pf - pc);
    rp += f * (Fine * pf - Coarse * pc);
    rx += u * c, ry += v * c, rz += w * c;
}
Curvature = sqrt(pow(rx,2) + pow(ry,2)) / rz;
Direction = atan2(ry,rx);
Phase     = atan2(sqrt(pow(rx,2) + pow(ry,2) + pow(rz,2)),rp);
Energy    = pow(rp,2) + pow(rx,2) + pow(ry,2) + pow(rz,2);
```
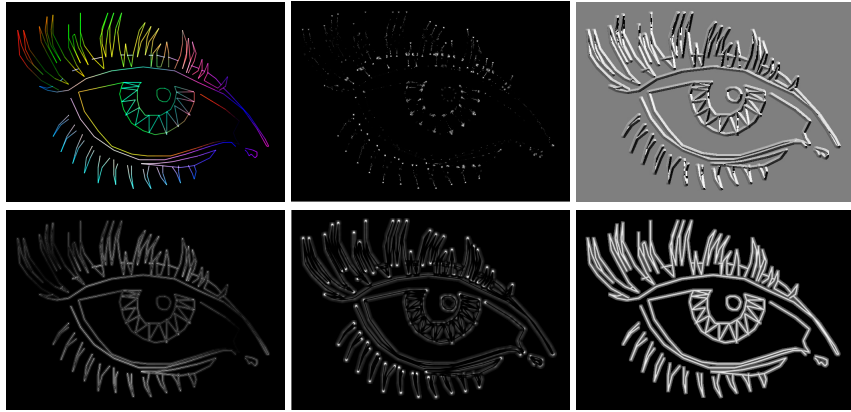
Fig. 7. Top row from left to right: Original signal, classical isophote curvature [12] and local direction information. Bottom row from left to right: *conformal monogenic signal* energy, curvature and phase. Note the observable illumination invariance of the conformal curvature and phase. Convolution mask size: 7×7 pixels.

5   Experimental Results

On synthetic signals with known ground truth the average error of the feature extraction converges to zero with increasing refinement of the convolution mask size. The advanced rotational invariance and isotropic behavior of the *conformal monogenic signal* curvature compared to the curvature delivered by the classical differential geometry approach can be seen clearly in figure 5. Under the presence of noise the *conformal monogenic signal* curvature performs more robust than e.g. the gradient based Sobel detector (see figure 8). Substituting the gradient and even the in [14] proposed phase constraints, the *conformal monogenic signal* curvature feature performs better in optical flow applications with an average angular error (AAE) of 1.99° compared to the best result $AAE = 2.67°$ achieved in [14] on the Yosemite sequence (see figure 8). Since the *conformal monogenic signal* combines all intrinsic dimensions in one framework it could be an interesting alternative for the gradient or the Laplace operator.

6   Conclusion

In this paper a new fundamental idea for locally analyzing 2D curved signals such as lines, edges, corners and junctions in one unified framework has been presented. It has been shown that the feature space can be extended by embedding 2D signals in higher dimensional conformal spaces in which the original 2D signal can be analyzed by generalized Hilbert transforms with more degrees of freedom. Without steering and in an rotational invariant way, local signal features such as phase, direction, energy and curvature can be determined in spatial domain by 2D convolution. The *conformal monogenic signal* can be computed
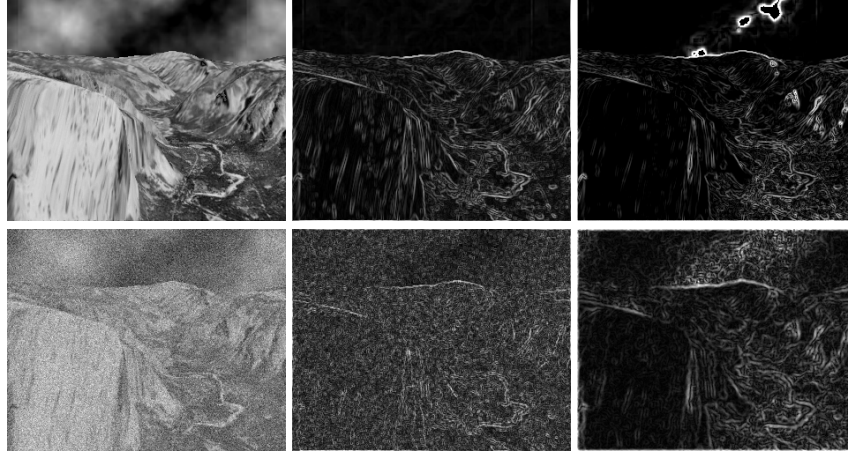
Fig. 8. Top row from left to right: Original Yosemite image, Sobel detector output and *conformal monogenic signal* curvature which delivers much more structural information (see cloudy sky). Bottom row from left to right: Noise degraded image (SNR=10dB), blurred Sobel output and *conformal monogenic signal* curvature. Convolution mask size: 7×7 pixels.
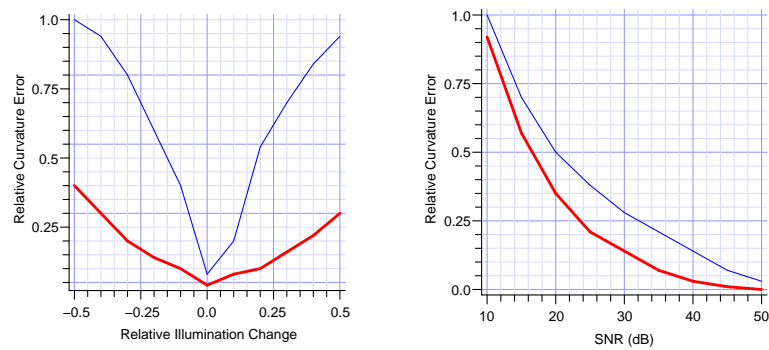

Fig. 9. Comparison of classical isophote curvature [12] (thin blue curve) and conformal curvature (thick red curve) errors. Left figure: Illumination change relatively to original signal. Right figure: Additive Gaussian noise. Convolution mask size: 5×5 pixels.

efficiently and easily implemented into existing low level image processing steps of Computer Vision applications. Furthermore exact curvature can be calculated with all the advantages of rotational invariant local phase based approaches (robustness against noise and illumination changes) and without the need of any derivatives. Hence, lots of numerical problems of partial derivatives on discrete grids can be avoided. All results can be proofed mathematically and by experiments. More applications of the *conformal monogenic signal* such as object tracking [12] by the conformal isophote curvature and the extension to image sequences will be part of future work.

References

1. Hahn, S.L.: Hilbert Transforms in Signal Processing. Artech House Inc, Boston, London (1996)
2. Felsberg, M., Sommer, G.: The monogenic scale-space: A unifying approach to phase-based image processing in scale-space. Journal of Mathematical Imaging and Vision **21** (2004) 5–26
3. Felsberg, M.: Low-Level Image Processing with the Structure Multivector, Technical Report No. 2016. PhD thesis, Kiel University, Department of Computer Science (2002)
4. Brackx, F., Knock, B.D., Schepper, H.D.: Generalized multidimensional Hilbert transforms in Clifford analysis. International Journal of Mathematics and Mathematical Sciences (2006)
5. Wietzke, L., Sommer, G., Schmaltz, C., Weickert, J.: Differential geometry of monogenic signal representations. In Sommer, G., ed.: Robot Vision. Volume 4931 of LNCS., Springer-Verlag, Berlin, Heidelberg, New York (2008) 454–465
6. Needham, T.: Visual Complex Analysis. Oxford University Press, Oxford (1997)
7. Toft, P.: The Radon Transform - Theory and Implementation. PhD thesis, Technical University of Denmark (1996)
8. Delanghe, R.: Clifford analysis: History and perspective. Computational Methods and Function Theory **1**(1) (2001) 107–153
9. do Carmo, M.P.: Differential Geometry of Curves and Surfaces. Prentice-Hall (1976)
10. Bernstein, S.: Inverse Probleme. Technical report, TU Bergakdemie Freiberg (2007)
11. Wietzke, L., Sommer, G.: The Conformal Monogenic Signal. In Rigoll, G., ed.: Pattern Recognition. Volume 5096 of LNCS., Springer-Verlag, Berlin, Heidelberg, New York (2008) 527–536
12. Lichtenauer, J., Hendriks, E.A., Reinders, M.J.T.: Isophote properties as features for object detection. CVPR (2) (2005) 649–654
13. Axler, S., Bourdon, P., Ramey, W.: Harmonic Function Theory (Graduate Texts in Mathematics). Volume 137. Springer (2002)
14. Zang, D., Wietzke, L., Schmaltz, C., Sommer, G.: Dense optical flow estimation from the monogenic curvature tensor. In: Scale Space and Variational Methods. Volume 4485 of LNCS., Springer-Verlag, Berlin, Heidelberg, New York (2007) 239–250